Analog of photon-assisted tunneling originated from dark Floquet state in periodically modulated waveguide arrays

Liping Li[1], Xiaobing Luo[2],* Xiaoxue Yang[1], Xin-You Lü[1],† and Ying Wu[1]‡
[1] *Wuhan National Laboratory for Optoelectronics and School of Physics, Huazhong University of Science and Technology, Wuhan, 430074, P. R. China and*
[2] *Department of Physics, Jinggangshan University, Ji'an 343009, P. R. China*
(Dated: January 13, 2016)

We theoretically report an analog of photon-assisted tunneling (PAT) in a periodically driven lattice array without a static biased potential by studying a three-channel waveguide system. This analog of PAT can be achieved by only periodically modulating the top waveguide and adjusting the distance between the bottom and its adjacent waveguide. It is numerically shown that the PAT resonances also exist in the five-channel waveguide system and probably exist in the waveguide arrays with other odd numbers of waveguides, but they will become weak as the number of waveguides increases. With origin different from traditional PAT, this type of PAT found in our work is closely linked to the existence of the zero-energy (dark) Floquet states. It is readily observable under currently accessible experimental conditions and may be useful for controlling light propagation in waveguide arrays.

PACS numbers: 42.65.Wi, 42.25.Hz

arXiv:1601.02829v1 [quant-ph] 12 Jan 2016

I. INTRODUCTION

Controlling quantum tunneling and transport through a periodic driving field has been a subject of intense studies in the last decades, for its relevance to fundamental physics tests as well as to great potential application in nanoscale devices[1, 2]. Among the most intriguing aspects of the subject, coherent destruction of tunneling (CDT)[3] and photon-assisted tunneling (PAT)[4] represent two seminal results. CDT is a resonant effect discovered in the pioneering work, in which the coherent tunneling between states is almost completely suppressed when the system parameters are carefully chosen at the isolated degeneracy point of quasi-energies[3]. It has so far generated great interests and has recently been observed experimentally in different physical systems[5, 6]. Recently, CDT has been found to occur over a wide range of system parameters in odd-N-state systems where one state is periodically driven with respect to others[7]. Such extension of destruction of tunneling to a finite parameter range, referred to as dark CDT, is attributed to the existence of localized dark Floquet state with zero quasi-energy[7, 8]. As the dark CDT was introduced in the high-frequency regime where the driving frequency is larger than all energy scales of the system, it naturally leads to certain interesting questions: whether the dark CDT and associated dark Floquet state still exist in the non-high-frequency regimes which are accessible by adjusting, for example, either the coupling strength between the neighboring states or the driving frequency? what new behaviors will emerge in the non-high-frequency regimes?

Photon-assisted tunneling (PAT) refers to a phenomenon in which tunneling contact disabled by a static tilt (dc bias potential) can be restored when the system exchanges energy of an integer number of photons with the oscillating field[9]. The static tilt (dc bias potential) leads to suppression of tunneling which is related to localized Wannier-Stark states[10]. When a multiple of the driving frequency of ac field matches the energy difference between adjacent rungs of the Wannier-Stark ladder, the system is able to absorb or emit photons with sufficient energy to bridge the energy difference created by the dc bias potential, through which tunneling is (partly) restored (PAT). So far, PAT has been experimentally observed in Josephson junctions[11], coupled quantum dots[12, 13], semiconductor superlattices [14, 15] and Bose-Einstein condensates in optical lattices[16].

In this article, we have studied the tunneling dynamics in lattice arrays with controllable boundary. Owing to the simplicity and flexibility offered by optical settings, the engineered photonic waveguides provide an ideal system for exploration of tunneling phenomena, in which spatial propagation of light mimics the temporal dynamics of a quantum particle in a lattice array[17, 18]. As illustrated in Fig.1, we present an optical implementation of our Hamiltonian in the form of a linear array of tunneling-coupled optical waveguides which is characterized in: (i) that the refractive index of the top boundary waveguide is modulated periodically along the propagation direction; and (ii) that the distance ωs_2 between the bottom boundary waveguide and its nearest neighbor is different from other identical nearest-neighboring spacings ωs_1. Thus, through adjustment of the distance ωs_2, the coupling strength between the bottom boundary waveguide and its nearest neighbor can be tuned to be sufficiently large in comparison to the modulation frequency. The role of photon is played by a periodic modulation of the the top boundary waveguide with a certain modulation frequency. Generally, PAT occurs in a system with a static biased potential which strongly suppresses usual Josephson oscillations. But here we report an analog of photon-assisted tunneling in a periodically driven lattice array without static tilt (dc bias potential) by comprehensively studying a three-channel waveguide system. Our numerical analysis discovers that dark CDT

*Electronic address: xiaobingluo2013@aliyun.com
†Electronic address: xinyoulu@gmail.com
‡Electronic address: yingwu2@126.com

(strong suppression of tunneling) and dark Floquet state still exist in the three-channel waveguide system even in the non-high-frequency regimes where the modulation frequency of the periodically modulated top waveguide is roughly equal to or smaller than the coupling strength between the bottom and its adjacent (middle) waveguide. However, when integer multiples of the modulation frequency approximately equal to the coupling strength between the bottom and its adjacent (middle) waveguide, the light tunneling from the top waveguide to the others is restored as a clear signature of photon-assisted tunneling. Different from the PAT observed in the earlier studies which usually requires a static biased potential to initialize the system in a self-trapped state, this type of PAT is closely linked to a dark Floquet state with zero quasi-energy. Our results are applicable for the five-channel waveguide system and also extendable to waveguide arrays with an odd number of waveguides.

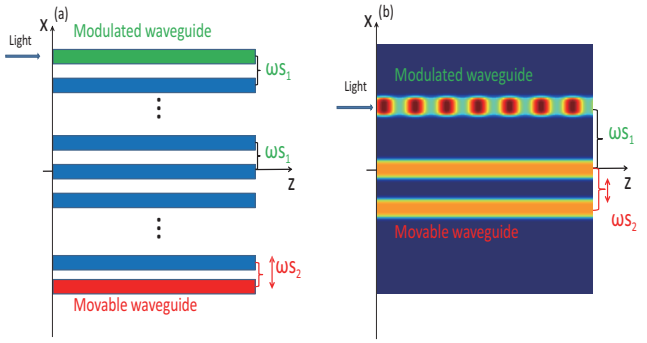

FIG. 1: (Color online) (a) Schematic of a tunneling-coupled optical waveguide array with controllable boundary that realizes an analog of photon-assisted tunneling. (b) A typical triplet waveguide system. The refractive index of the top boundary waveguide is modulated periodically along the propagation direction. The space separation between the bottom boundary waveguide and its nearest neighbor ωs_2 is adjustable by moving the bottom boundary waveguide towards the other waveguides, while the spacings ωs_1 between other nearest-neighboring waveguides are fixed.

II. LIGHT TUNNELING DYNAMICS IN MODULATED PHOTONIC LATTICES WITH CONTROLLABLE BOUNDARY

We now discuss light dynamics in a photonic structure composed of an array of waveguides, in which the refractive index of the top boundary waveguide is modulated periodically along the propagation direction and the distance between the other boundary waveguide and its nearest neighbor is adjustable, as schematically illustrated in Fig.1. The coupled-mode equations describing the beam dynamics in such structures can be written as

$$\begin{aligned} i\frac{da_1}{dz} &= \sigma(z)a_1 + \Omega_1 a_2, \\ i\frac{da_j}{dz} &= \Omega_1 a_{j-1} + \Omega_1 a_{j+1}, \quad (j = 2, 3, ..., N-2) \\ i\frac{da_{N-1}}{dz} &= \Omega_1 a_{N-2} + \Omega_2 a_N, \\ i\frac{da_N}{dz} &= \Omega_2 a_{N-1}, \end{aligned} \tag{1}$$

where a_j is field mode amplitude in the j-th waveguide, z the propagation distance, Ω_1 the coupling strength between neighboring waveguides with spacing ωs_1, Ω_2 the coupling strength between the bottom boundary waveguide ($j = N$) and its adjacent waveguide ($j = N-1$), and $\sigma(z)$ the normalized difference between the propagation constants of the top boundary waveguide and the other waveguides of the array. We consider a harmonic modulation of the linear refractive index of the top boundary waveguide along the propagation direction with $\sigma(z) = A\sin(\omega z)$, where A is the relative depth of the harmonic longitudinal modulation, and ω is the spatial modulation frequency. In a different perspective, the above equation (1) can be regarded as describing the system of a quantum wave in a periodically driven lattice array if z is viewed as time t.

As is well known, the periodic time-dependent equation (1) admits solutions in the form of Floquet states $(a_1, a_2, ..., a_N)^T = (\tilde{a}_1, \tilde{a}_2, ..., \tilde{a}_N)^T \exp(-i\varepsilon z)$, where ε is the quasi-energy and the amplitudes $(\tilde{a}_1, \tilde{a}_2, ..., \tilde{a}_N)^T$ are periodic with modulation period $T = 2\pi/\omega$. Our analysis is based on the Floquet theory which offers a powerful tool for the treatment of the periodically driven system.

In the case of $\Omega_1 = \Omega_2$, the equation (1) is reduced to the one discussed in Refs. [7, 8], where a significant suppression of tunneling (the so-called dark CDT) exists for a wide range of system parameters in all odd-N-state systems with identical coupling constants because of occurrence of the zero-energy (dark) Floquet state. The case of $\Omega_1 \neq \Omega_2$ has yet been explored. In this work, we will focus on that case and give two example models (three- and five-waveguide systems) to explore new physics in these systems.

A. PAT in three-guide system

We start our consideration for the three-guide system, the minimal one for odd-N-state systems. In this case, the dynamical equations are of the form

$$\begin{aligned} i\frac{da_1}{dz} &= A\sin(\omega z)a_1 + \Omega_1 a_2, \\ i\frac{da_2}{dz} &= \Omega_1 a_1 + \Omega_2 a_3, \\ i\frac{da_3}{dz} &= \Omega_2 a_2. \end{aligned} \tag{2}$$

To study the system's beam dynamics, we solve numerically the coupled-mode equation (2) with the light initially localized in the 1-th waveguide (the top boundary waveguide). With the numerical solution, we compute the intensity of light

staying in the initial waveguide by $P_1(z) = |a_1(z)|^2$ and measure the minimum value of $P_1(z)$ over a long-enough propagation distance. When Min(P_1) is not zero, the tunneling is suppressed as the light is not allowed to be fully transferred from the 1-th mode (guide) to the other modes (guides). In Fig.2(a), we display Min(P_1) versus the coupling strength Ω_2 at the fixed parameters $A = 6.6, \omega = 3, \Omega_1 = 1$. For $\Omega_2 = 0$, the system is in fact a two-guide system in which the conventional CDT happens only at the isolated degeneracy point of the quasi-energies, and consequently Min(P_1) takes a zero value because our driving parameter is set to be slightly off the isolated degeneracy point. When Ω_2 is increased from zero, the value of Min(P_1) becomes relatively large except at a series of very sharp dips. In general, periodic modulation of the top boundary waveguide will yield a significant suppression of the light tunneling in the three-guide system even with $\Omega_1 \neq \Omega_2$, as shown in Fig.2(a). However, at particular values of the coupling strength Ω_2, $\Omega_2 \approx n\omega$ with n being integer, the value of Min(P_1) exhibits a series of sharp dips, in analogy to the n-photon-like resonances which destroy the effect of suppression of tunneling. It also can be observed that as the coupling strength Ω_2 is increased, the higher photon-like resonances become very weak and thus are almost not visible.

For a deep insight into the tunneling dynamics obtained in Fig.2(a), we numerically compute the quasi-energies and Floquet states of this system as shown in Fig.2(b)-(c). As shown in Fig.2(b), this three-state system always possesses a Floquet state with zero quasi-energy regardless of the value of Ω_2. The other two quasi-energies make a set of close approaches to each other as Ω_2 is increased. At the points of close approach, namely, at $\Omega_2 \approx n\omega$, the value of Min(P_1) displays sharp dips and the tunneling is significantly restored. We also plot the time-averaged population distribution $\langle P_j \rangle = (\int_0^T dz|a_j|^2)/T$ for the zero-energy Floquet state $(a_1, a_2, a_3)^T$ in Fig.2(c). Considering that the dynamics is determined by the Floquet state, self-trapping (suppression of tunneling) of light intensity initially populating at the 1-th mode (guide) will take place if $\langle P_1 \rangle > 0.5$ holds. As seen in Fig.2(c), the zero-energy Floquet state has negligible population at the central mode (guide) while the population $\langle P_1 \rangle$ is much larger than 0.5 for all values of Ω_2 except those in the vicinity of $\Omega_2 \approx n\omega$. Correspondingly, suppression of tunneling (CDT) occurs for all values of Ω_2 except the locations of photon resonances, as shown in Fig.2(a). The Floquet state with zero quasi-energy is essentially the dark Floquet state, not only for its zero quasi-energy but also for its negligible population at the central waveguide; the suppression of tunneling (CDT) is of the dark CDT as it is caused by the dark Floquet state rather than level degenaracy. In fact, the CDT-PAT transition found in Fig.2(b) is closely related to the sharp localization-delocalization transition of population $\langle P_1 \rangle$ for the zero-energy (dark) Floquet state. Note that the dark Floquet originally discovered and defined in the high-frequency limit can be reduced to the well-known dark state by means of high-frequency averaging method[7, 8]. In this considered model (2), however, the dark Floquet state and the associated CDT can still exist in the non-high-frequency regimes where the coupling strength Ω_2 is much larger than the modulation frequency and the high-frequency averaging method is invalid. These results will greatly enrich our understanding of dark Floquet state and dark CDT.

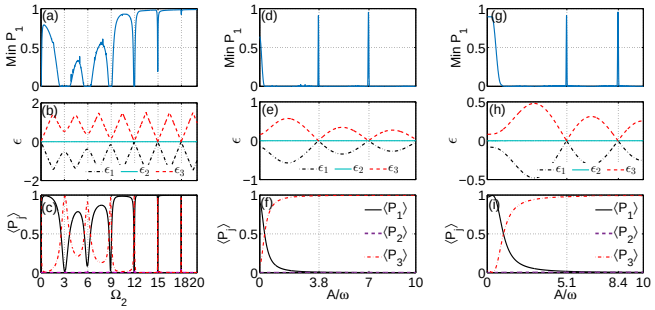

FIG. 2: (Color online) PAT in three-guide optical system. The left column: (a) the minimum value of intensity of light at the initially populated guide-1, Min(P_1) versus Ω_2, with $A = 6.6, \omega = 3, \Omega_1 = 1$; (b) the corresponding quasi-energy ϵ versus Ω_2 and (c) the time-averaged population $\langle P_j \rangle$ belonging to the zero-energy (dark) Floquet state versus Ω_2. The middle column: (d) Min(P_1) versus A/ω for the 1-photon resonance $\omega = 3, \Omega_2 = 3, \Omega_1 = 1$; (e) the corresponding quasi-energy ϵ versus A/ω and (f) the time-averaged population $\langle P_j \rangle$ belonging to the zero-energy (dark) Floquet state versus A/ω. The right column: (g) Min(P_1) versus A/ω for the 2-photon resonance $\omega = 3, \Omega_2 = 6, \Omega_1 = 1$; (h) the corresponding quasi-energy ϵ versus A/ω and (i) the time-averaged population $\langle P_j \rangle$ belonging to the zero-energy (dark) Floquet state versus A/ω.

In Fig.2(d), we show how the value of Min(P_1) varies under conditions that the modulation amplitude is increased, while its frequency is held constant at $\omega = 3$ and the coupling strength held $\Omega_2 = \omega, \Omega_1 = 1$. This corresponds to the $n = 1$ photon resonance. For $A = 0$, the system is self-trapped in the 1-th waveguide due to the existence of an imbalanced dark state $(-\Omega_2/\Omega_1, 0, 1)^T$ with $\Omega_2/\Omega_1 > 1$, and thus the value of Min(P_1) is nonzero. When the periodic driving is applied, as A is increased from zero, the value of Min(P_1) rapidly drops to zero, which indicates that the photon resonance destroys the self-trapping effect. When A/ω is increased further, Min(P_1) takes extremely low values about zero except at a sequence of very narrow peaks. These peaks are precisely centered at $A/\omega = 3.83, 7.01, ...$, the zeros of $J_1(A/\omega)$. In Fig.2(e)-(f), we plot the quasi-energies and the population distributions of the dark Floquet state for the first photon resonance ($n = 1$). Apparently, the quasi-energies are degenerate when $J_1(A/\omega) = 0$, and when away from $A = 0$ the dark Floquet state has averaged population at the 1-th mode (guide) well below the value of 0.5. Therefore it can be concluded that the well-defined quasienergy crossings instead of the dark Floquet state are the origin of the extremely sharp peaks seen in Fig.2(d).

In Fig.2(g), we show the values of Min(P_1) in the three-guide optical system for the $n = 2$ resonances. As is expected, the values of Min(P_1) exhibit a number of extremely sharp peaks centered on the zeros of $J_2(A/\omega)$ where the quasi-energies will be degenerate; see Fig.2(h). Similar to the case of $n = 1$ resonance, the sharp peaks in the $n = 2$ resonance is also caused by the level degeneracy rather than the dark Floquet state, as it is shown in Fig.2(i) that the population $\langle P_1 \rangle$ corresponding to the dark Floquet state is well below 0.5 at

the points of quasi-energy crossings.

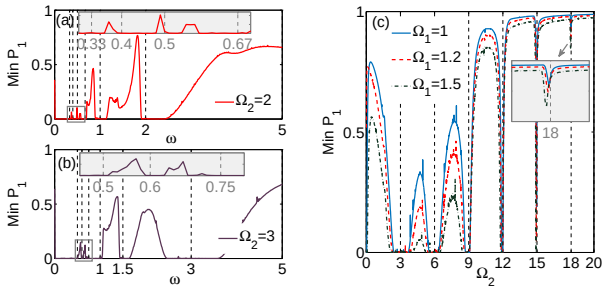

FIG. 3: (Color online) (a)-(b)The minimum value of population distribution P_1, Min(P_1), as a function of the modulation frequency ω with $\Omega_2 = 2$ and $\Omega_2 = 3$ respectively. Other parameters are chosen as $\Omega_1 = 1$ and $A = 6.6$. (c)Min(P_1) versus Ω_2 with different values of Ω_1. Other parameters are chosen as $\omega = 3$ and $A = 6.6$.

In order to observe the n-photon-like resonances from a different angle, we also plot Min(P_1) as a function of the modulation frequency ω for two fixed parameters $\Omega_2 = 2$ and $\Omega_2 = 3$ in Fig.3 (a) and (b) respectively. We can readily observe that the n-photon-like resonances occur at comparatively broad intervals around $\omega = \Omega_2/n$. The width of such photon-assisted tunneling resonances is much larger than those of PAT resonances observed in the literature. We now elaborate the physics underlying this photon-assisted tunneling resonances. The actual resonance condition does not refer directly to $\Omega_2 = n\omega$ but rather to the tunneling frequency of the model (2) without periodic modulation. The unmodulated three-guide optical system (2) admits three energy level as $0, \pm\sqrt{\Omega_1^2 + \Omega_2^2}$, and the space of two neighboring energy levels is $\omega_0 = \sqrt{\Omega_1^2 + \Omega_2^2}$. In such a system, the existence of imbalanced dark state with zero energy results in the suppression of tunneling when the periodic modulation is switched off. The periodic modulation effectively creates "photons" that bridge the energy gap between neighboring energy levels. Thus, a photon-assisted tunneling resonance can occur at a modulation frequency which satisfies the resonance condition $\omega_0 = n\omega$. When Ω_2 is considerably larger than Ω_1, the energy difference ω_0 of the unmodulated system will become principally characterized by Ω_2 and therefore the resonance condition is approximately given by $\Omega_2 = n\omega$. As clearly seen in the inset in Fig.3 (c), the position of n-photon-like resonance does slightly shift with increasing Ω_1 due to the dependence of the energy difference (tunneling frequency) ω_0 on Ω_1.

B. PAT in five-guide system

We now turn to the case of the five-guide optical system where the dynamical equations are

$$
\begin{aligned}
i\frac{da_1}{dz} &= A\sin(\omega z)\, a_1 + \Omega_1 a_2, \\
i\frac{da_j}{dz} &= \Omega_1 a_{j+1} + \Omega_1 a_{j-1}, \quad j = 2, 3 \\
i\frac{da_4}{dz} &= \Omega_1 a_3 + \Omega_2 a_5, \\
i\frac{da_5}{dz} &= \Omega_2 a_4. \qquad (3)
\end{aligned}
$$

The dynamics for the five-guide system are investigated by direct integration of the time-dependent Schrödinger equation (3) with the light initially localized at the guide 1. In Fig.4, we show the value of Min(P_1) as a function of Ω_2 which exhibits a sequence of PAT resonances with similar behavior as that of a three-guide system. The higher n-photon resonances with $n \geq 3$ become very weak, almost invisible, as illustrated in the inset of Fig.4 (a). By comparison of Fig.2 (a) with Fig.4 (a), it is apparent that the same order PAT resonance for the five-guide system is much narrower and weaker than for the three-guide system. Like the case of the three-guide system, this five-guide system also possesses a dark Floquet state with zero quasi-energy and negligible population at all of the even j-th guides (modes), as illustrated in Figs.4(b) and (c). Reason for the existence of the analog of PAT resonances in the five-guide system lies in that population distribution $\langle P_1 \rangle$ for the dark Floquet state simultaneously displays a series of sharp dips at the positions of PAT resonances [see Figs.4(c)].

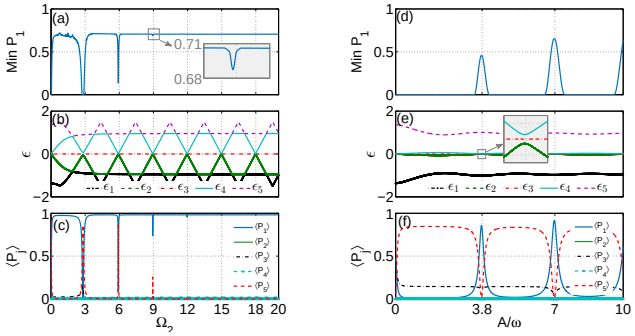

FIG. 4: (Color online) PAT in five-guide optical system. The left column: (a) the minimum value of population distribution at guide 1, Min (P_1), versus Ω_2 with $A = 6.6, \omega = 3, \Omega_1 = 1$; (b) the corresponding quasi-energy ϵ versus Ω_2 and (c)the time-averaged population $\langle P_j \rangle$ belonging to the zero-energy (dark) Floquet state versus Ω_2. The right column: (d) Min(P_1) versus A/ω for the 1-photon resonance $\omega = 3, \Omega_2 = 2.8, \Omega_1 = 1$; (e) the corresponding quasi-energy ϵ versus A/ω and (f) the time-averaged population $\langle P_j \rangle$ belonging to the zero-energy (dark) Floquet state versus A/ω.

In Fig.4(d), we plot Min(P_1) obtained in the five-guide system as a function of the modulation parameter A/ω for the 1-photon resonance $\Omega_2 = 2.8, \omega = 3, \Omega_2 \approx \omega$. As discussed before, we can observe that the values of Min(P_1) are peaked at the zeros of $J_1(A/\omega)$, at which CDT occurs, while between the peaks Min(P_1) take extremely low values as result of PAT. However, compared with the case of three-guide system, the

peaks in Min(P_1) are considerably lower and broader. As can be clearly seen from Figs.4(e) and (f), the peaks in Min(P_1) are indeed centered at the points of closest approach of the quasi-energies where the dark Floquet state has a population $\langle P_1 \rangle > 0.5$. The numerical results establish again a firm link between PAT and dark Floquet state in our considered systems.

C. Tunneling dynamics in the four- and six-guide optical systems and beyond

Finally, we briefly discuss the case of the four- and six-guide systems. The dynamics for $N = 4$ and $N = 6$ are presented in Fig.(5) on the basis of a full numerical analysis of equation (1) with the light initially populated in the guide 1. It tells the existence of a sharp transition from CDT to complete tunneling for both cases of $N = 4$ and $N = 6$ when the coupling strength Ω_2 is increased from zero. A close examination of the tunneling dynamics at $\Omega_2 = n\omega$ shows that the value of Min(P_1) displays narrow peaks nearly at zeros of $J_0(A/\omega)$ where a pair of quasi-energies become degenerate. This closely resembles the case of the high-frequency modulation $\omega \gg \max(\Omega_1, \Omega_2)$ where CDT is dominated by the zeros of $J_0(A/\omega)$. As shown in Figs.(5) (b) and (e), the localization centered nearly at zeros of $J_0(A/\omega)$ is fairly smaller for the four-guide system, but still generates high peaks for the six-guide system.

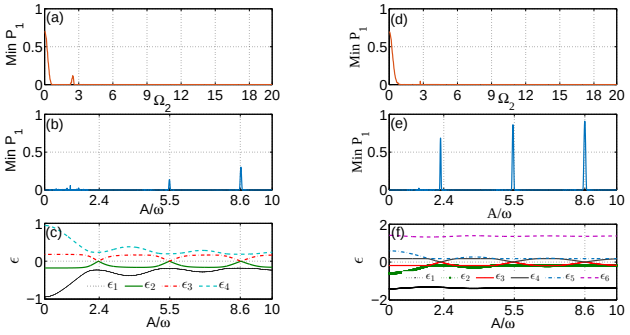

FIG. 5: (Color online) The left column: the characteristics of four-guide optical system; The right column: the characteristics of six-guide optical system. (a) and (d): Min(P_1) versus Ω_2 at $A = 6.6, \omega = 3, \Omega_1 = 1$; (b) and (e): Min($P_1$) versus A/ω at $\Omega_2 = 3, \omega = 3, \Omega_1 = 1$; (c) and (f): quasi-energies ε versus A/ω at $\Omega_2 = 3, \omega = 3, \Omega_1 = 1$.

Moreover, we have simulated multiwaveguide systems of other numbers of waveguides. The numerical results, which are not displayed here, show that the PAT resonances probably occur in all the odd-N-guide optical systems, while the PAT resonances become weaker with the increase of number of guides. However, all the even-N-guide optical systems exhibit CDT to complete tunneling transition without appearance of n-photon-like resonance when the coupling strength Ω_2 is increased from zero, which is totally different from the case of odd-N-guide system.

III. POSSIBILITY OF EXPERIMENTAL REALIZATION

Now, we discuss the experimental possibility of observing our theoretical predictions based on the coupled-mode equations. A more rigorous dynamics for our system can be simulated by the Schrödinger equation for the dimensionless field amplitude E, which describes the light propagation along the z axis of an array of N waveguides

$$i\frac{\partial E}{\partial z} = -\frac{1}{2}\frac{\partial^2 E}{\partial^2 x} - pR(x,z)E. \tag{4}$$

Here x and z are the normalized transverse and longitudinal coordinates, and p describes the refractive index contrast of the individual waveguide. For our system, the refractive index of the first waveguide is harmonically modulated along the propagation direction, while all other $N-1$ waveguides are unmodulated. The corresponding refractive index distribution of this kind of waveguide system is given by

$$\begin{aligned} R(x,z) &= \sum_{j=-(N-2)}^{1} [1 + f_j(z)] \exp\left[-\left(\frac{x - jw_j}{w_x}\right)^6\right], \\ f_1(z) &= \mu \sin(\omega z), \quad f_j(z) = 0 (j \neq 1), \end{aligned} \tag{5}$$

with the position of each waveguide being jw_j, the channel width w_x, the longitudinal modulation amplitude μ, and the modulation frequency ω. Therein the super-Gaussian function $\exp(-x^6/w_x^6)$ describes the profile of a single waveguide with width w_x. In our discussion, all the waveguide spacings $[jw_j - (j-1)w_{j-1}]$ are identical except that the spacing between the bottom boundary waveguide and its neighbor is variable.

In what follows, we will illustrate our main results with a triplet waveguide system ($N = 3$) by directly integrating the field propagation equation (4) with realistic experimental parameters. We set $w_x = 0.3, p = 2.78, \mu = 0.2$ and $\omega = 3.45 \times (\pi/100)$. We characterize two distinct waveguide spacings as ws_1 and ws_2 respectively, where $ws_1 = w_1$ stands for the separation between the top waveguide and the middle waveguide and $ws_2 = w_{-1}$ the separation between the bottom waveguide and the middle waveguide. Further we set $ws_1 = 3.2$ and choose different values of ws_2 to observe PAT resonance. As in the experiments[19, 20], w_x and w_j are in units of 10 μm, and $p = 2.78$ corresponds to a real refractive index of 3.1×10^{-4}. In all simulations we excited the top channel at $z = 0$, using the fundamental linear mode of the isolated waveguide. It is instructive to normalize the modulation frequency to the beating frequency of the unmodulated linear dual-core coupler with spacing ws_1, $\Omega_b = 2\Omega_1 = 2\pi/T_b$, where T_b is a beating period representing the shortest distance for the light returning to the input waveguide. For our set of parameters one has $T_b = 100$ and thus $\omega = 3.45\Omega_1$.

The beam dynamics of a three-guide optical system are visualized in Fig.(6) for three values of ws_2, which firmly verifies the predictions from the coupled-mode equation (2). It can be readily observed from Figs.(6) (a) and (b) that the light tunneling is almost completely suppressed, as the three-channel waveguide system has equal channel spacing $ws_1 =$

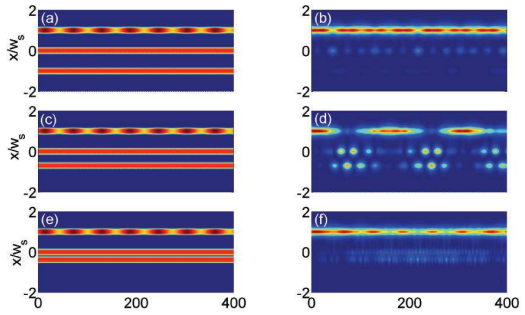

FIG. 6: (Color online) Light propagation in three-guide optical systems with different spacings between the bottom and the middle waveguide for the input beam centered at the top waveguide. First row: (a) and (b): the refractive index distribution $R(x,z)$ and the light propagation $|E(x,z)|^2$ for a three-guide system with equal channel spacing $ws_1 = ws_2 = 3.2$; Second row: (c) and (d): the refractive index distribution $R(x,z)$ and the light propagation $|E(x,z)|^2$ for a three-guide system with unequal channel spacing $ws_1 = 3.2, ws_2 = 2.22$; Third row: (e) and (f): the refractive index distribution $R(x,z)$ and the light propagation $|E(x,z)|^2$ for a three-guide system with unequal channel spacing $ws_1 = 3.2, ws_2 = 1.2$.

$ws_2 = 3.2$. At $ws_2 = 2.22$, the light coupling between the waveguide channels is restored [see Fig.(6) (c) and (d)]. The revival of light tunneling is a signature of PAT resonance predicted by the coupled-mode theory. In fact, our numerical simulation (not shown here) reveals that the beating period of an unmodulated linear dual-core coupler with a channel spacing 2.22 is about $100/3.45$. As such, we have $\Omega_2 \approx 3.45\Omega_1$ and $\Omega_2 \approx \omega$, which is in fact the position of the first photon resonance. As the channel spacing ws_2 is reduced further, it is expectable to observe again the strong suppression of light tunneling[see Fig.(6) (e) and (f)]. These results are in good qualitative agreement with those in Fig.2(a) based on the coupled-mode equation.

IV. CONCLUSION

In summary, we have theoretically reported an analog of PAT in a three-channel waveguide system, in which the space separation between the bottom and the middle waveguides is adjustable and the refractive index of the top waveguide is modulated periodically along the light propagation direction. With the standard coupled-mode theory, the system can be described by a driven three-state discrete model with two distinct coupling strengths Ω_1 and Ω_2, where Ω_1 stands for the coupling strength between states 1 and 2, and Ω_2 between states 2 and 3. In studying the three-state discrete model, we have found that (i) a strong suppression (CDT) associated with the zero-energy (dark) Floquet state persists even in the non-high-frequency modulation regimes where $\omega \leq \max(\Omega_1, \Omega_2)$ except at a series of resonance positions; (ii) at particular values of the coupling strength Ω_2, $\Omega_2 \approx n\omega$ with n being integer, the tunneling dynamics is (partly) restored, analogous to the n-photon-like resonances which overcome the effect of suppression of tunneling. The numerical calculations illustrate that the PAT resonances exist in the five-state system and also probably exist in the systems with arbitrary odd number of coupled states. In particular, the PAT resonances will become weaker with the increase of number of states (modes). This type of PAT found in our work has a different origin from traditional PAT. It is closely related to the existence of the dark Floquet state. The main results are demonstrated by the direct numerical simulations of propagation dynamics based on the full continuous model with realistic experimental parameters, which indicates that the PAT found in our work can be readily tested in the current experimental setup.

Acknowledgments

The work is supported in part by the National Fundamental Research Program of China (Grant No. 2012CB922103), the National Science Foundation (NSF) of China (Grant Nos. 11375067, 11275074, 11374116, 11204096, 11405061 and 11574104), the Fundamental Research Funds for the Central Universities, HUST (Grant No. 2014QN193). X. Luo is also partially supported by the NSF of China under Grants 11465009, 11165009, the Program for New Century Excellent Talents in University of Ministry of Education of China (NCET-13-0836), Scientific and Technological Research Fund of Jiangxi Provincial Education Department under Grant No. GJJ14566, and the financial support provided by the Key Subject of Atomic and Molecular Physics in Jiangxi Province. X. Luo thanks Prof. Biao Wu for his supports over the years.

[1] M. Grifoni and P. Hänggi, Phys. Rep. **304**, 229 (1998).
[2] G. Platero and R. Aguado, Phys. Rep. **395**, 1 (2004).
[3] F. Grossmann, T. Dittrich, P. Jung and P. Hänggi, Phys. Rev. Lett. **67**, 516 (1991).
[4] P. K. Tien and S. R. Gordon, Phys. Rev. **129**, 647 (1963).
[5] G. Della Valle, M. Ornigotti, E. Cianci, V. Foglietti, P. Laporta and S. Longhi, Phys. Rev. Lett.**98**, 263601 (2007).
[6] E. Kierig, U. Schnorrberger, A. Schietinger, J. Tomkovic, and M. K. Oberthaler, Phys. Rev. Lett. **100**, 190405 (2008).
[7] X. Luo, L. Li, L. You, and Biao Wu, New J. Phys. **16**, 013007 (2014).
[8] L. Li, X. Luo, X. Lü, X. Yang, and Y. Wu, Phys. Rev. A **91**, 063804 (2015)
[9] A. Eckardt, T. Jinasundera, C. Weiss, and M. Holthaus, Phys. Rev. Lett. **95**, 200401 (2005).
[10] M. Glück, A. R. Kolovsky, and H. J. Korsch, Phys. Rep. **366**, 103 (2002).
[11] S. Shapiro, Phys. Rev. Lett. **11**, 80 (1963).
[12] L. P. Kouwenhoven, S. Jauhar, J. Orenstein, and P. L. McEuen, Phys. Rev. Lett. **73**, 3443 (1994).
[13] T. H. Oosterkamp, L. P. Kouwenhoven, A. E. A. Koolen, N. C. van der Vaart, and C. J. P. M. Harmans, Phys. Rev. Lett. **78**,

1536 (1997).
[14] P. S. S. Guimaraes, B.J. Keay, J. P. Kaminski, S.J. Allen, Jr., P. F. Hopkins, A. C. Gossard, L. T. Florez, and J.P. Harbison, Phys. Rev. Lett. **70**, 3792 (1993).
[15] B. J. Keay, S. J. Allen, Jr., J. Galán, J. P. Kaminski, K. L. Campman, A. C. Gossard, U. Bhattacharya, and M. J. W. Rodwell, Phys. Rev. Lett. **75**, 4098 (1995).
[16] C. Sias, H. Lignier, Y. P. Singh, A. Zenesini, D. Ciampini, O. Morsch and E. Arimondo, Phys. Rev. Lett. **100**, 040404 (2008).
[17] I. L. Garanovich, S. Longhi, A. A. Sukhorukov, and Y. S. Kivshar, Phys. Rep. **518**, 1 (2012).
[18] S. Longhi, Laser Photon. Rev. **3**, 243 (2009).
[19] A. Szameit, Y. V. Kartashov, M. Heinrich, F. Dreisow, R. Keil, S. Nolte, A. Tünnermann, V. A. Vysloukh, F. Lederer and L. Torner, Opt. Lett. **34**, 2700 (2009).
[20] A. Szameit, Y. V. Kartashov, F. Dreisow, M. Heinrich, T. Pertsch, S. Nolte, A. Tünnermann, V. A. Vysloukh, F. Lederer, and L. Torner, Phys. Rev. Lett. **102**, 153901 (2009).